Iran University of Science and Technology

Automotive Science and Engineering

Journal Homepage: ase.iust.ac.ir

ISSN: 2008-9899

Torsional and bending stiffness and modal analysis of a bus structure

Zahra Taghizade[1], Mohammad yaghoobian[2], Javad Marzbanrad[3*]

[1] M.Sc, School of Automotive Engineering, Iran University of Science and Technology, Tehran, Iran

[2] PhD, Department of mechanical engineering, Isfahan university,Isfahan,Iran

[3] Professor, School of Automotive Engineering, Iran University of Science and Technology, Tehran, Iran

ARTICLE INFO

Article history:

Received :18 Mar 2024

Accepted: 2 Jun 2024

Published:26 Jul 2024

Keywords:

Bending

Torsional

Bus structure

Modal analysis

Static linear analysis

A B S T R A C T

A bus experiences various loads during operation, stressing its structural components and causing noise, vibrations, and strains. To withstand these stresses, components must have sufficient stiffness, strength, and fatigue properties. In this study, the CAD model of a bus was created in SolidWorks and meshed using HyperMesh. A modal analysis conducted in HyperMesh verified the model's integrity, welding joint accuracy, and suitability for further analysis. A HyperMesh solver performed bending and torsional analyses. The torsional and bending stiffness of the bus body was calculated based on these results. Previous research primarily focused on stress and displacement, neglecting torsional and bending stiffness analysis for three-axle buses. This study addresses this gap, providing industry engineers with insights into acceptable torsional and bending stiffness for intercity buses. This knowledge supports the design of buses with adequate braking and turning capabilities. Additionally, the research contributes to bus body optimization efforts. In subsequent studies, scientists can experiment with various materials and models of various bus structure beam profiles.

1. Introduction

The longevity, cost, and safety performance of a bus body are directly influenced by its design [1]. A crucial component of passenger vehicle performance is the bus body frame [2]. Important factors to consider are the bus structure's torsional and bending stiffness. Two primary goals for a bus's components are to reduce weight and maintain an appropriate level of torsional stiffness. Whereas high torsional stiffness increases vehicle safety, handling, and passenger comfort, weight reduction increases fuel efficiency. The topic of optimizing torsional and bending stiffness has been extensively researched. Modified beam gauges have been used to optimize bus weight [3]. Additionally, simplified finite element modeling for cars has been proposed, substituting one-dimensional beams and panels with large cross-sections for load-

*Corresponding Author
Email Address: marzban@iust.ac.ir
https://doi.org/.22068/ase.2024.680

[DOI: 10.22068/ase.2024.680]

bearing components [4]. Body frame stiffness and static strength analysis computed under various working conditions, including bending and torsion, revealed maximum stress values within allowable limits [5]. Weight reduction can be achieved through Component Thinning. Studies have also investigated the impact of the roof frame on stiffness and weight by comparing a single-body design with a separate roof frame connected by steel elements and panels [6]. The influence of side stiffening panels on the stiffness of the bus construction has been explored [7]. The amount of bending stress, etc., is calculated using beam-related calculations that treat the chassis as a beam. The simulation results were compared to the computational results, and the comparison was positive [8]. Studies have focused on improving torsional stiffness by designing and simulating chassis deflection using the finite element method [9]. Several chassis designs were presented, and the multi-hole model was found to have the highest torsional strength, making it the preferred choice [9]. An engineering method has been developed to replace the vehicle model's structural elements with those of the concept model [10]. This conceptual model accurately predicted bending and torsional stiffness compared to the original model [11]. Response surface optimization (RSO) was used for both pure bending and torsion loading scenarios. This method increased the optimized model's torsional stiffness by 3.29% (51.07 Nm/°) and reduced its weight by 2.64% [12]. Two stiffness analysis methods were performed, considering the vehicle wheelbase and spring bracket loading. The spring bracket approach closely matched actual results and was 5.4 times more accurate than the wheelbase method [13]. A method for improving bus stiffness involved optimizing the cross-sectional characteristics of the main body components while maintaining the base model's weight [14]. Numerical analysis of the bus body frame's structure during braking and cornering led to a 3.07% weight reduction through frame optimization [15]. The technique used for lightweight design involves optimizing topology and reducing the number of frame elements [16]. Due to the lack of previous studies on torsional and bending stiffness, this study investigated vertical bending and torsional stiffness and conducted a modal analysis of the three-axle bus. The accuracy of the results was verified through comparison with existing literature.

Flexural and Torsional Strength Analysis

The chassis typically withstands four main types of loads:

a) Vertical bending: When the weight of passengers, baggage, and vehicle components is concentrated in the middle between the two axles, and the chassis is supported at both ends by axles, the longitudinal beams of the chassis undergo vertical bending. This causes the middle section of the chassis to flex. If both front wheels hit a pothole simultaneously, the chassis can bend in this way [17].

b) Longitudinal torsion: When the front and rear wheels of the chassis come into contact with an object at an angle at the same time, they rotate in opposite directions [17]. This causes longitudinal torsion in both the longitudinal and lateral elements of the chassis, resulting in chassis deformation. The maximum torsion occurs in this case. The chassis must be strong enough to withstand the torque caused by a wheel hitting an obstruction. The vehicle's resistance to torsion determines the acceptable torsional torque when driving over road impediments (such as speed bumps).

c) Lateral bending: The chassis may experience lateral forces due to crosswinds, road imperfections, road camber, or

[DOI: 10.22068/ase.2024.680]

centrifugal forces during cornering. These lateral forces, countered by tire-road adhesion, cause torsion in the lateral elements of the chassis and lead to chassis deformation [17].

d) Horizontal distortion: When a chassis frame moves forward or backward, it encounters potholes, junctions, bumps, and surface curbs through wheel impacts, causing the front of the chassis to deform into a parallelogram.

2.1 Bending Flexibility

It is evident from doing a particular static test in which just the transfer forces and displacements are involved that all of the forces F_n operating on the structure can be described as a general force F plus a number of coefficients that vary according to the force's size and geometry.

$$F_n = X_n F \quad (1)$$

$$\sum_n x_n = 0 \quad (2)$$

An analogous approach can be used to write tests involving torque and torsion pairs. The following d_n displacements at the location where the load and supports are applied are also used to determine the static flexibility of C:

$$C = \frac{\sum_n X_n d_n}{F} \quad (3)$$

The following equation obtains the contribution of each vibration mode from the flexibility of C [18]:

$$C = \frac{\Sigma_i \Sigma_j X_i X_j \psi_i \psi_j}{m(2\pi f)^2} \quad (4)$$

Where m is the modal mass, f is the amplification frequency, and ψ_i is the form of the modes at the location of load application and supports.

The sum of each softness of the modes also yields the total softness. One may obtain the total of all distributed modes by inducting a "soft" transfer function to 0 Hz. The following is the flexibility function:

$$\frac{d}{F} = \Sigma_i \Sigma_j X_i X_j \frac{di}{Fj} = -\frac{1}{(2\pi f)^2} \Sigma_i \Sigma_j X_i X_j \frac{a_i}{F_j} \quad (5)$$

This article states that the transfer function is not included in the intermediate function below at frequency 0 Hz, which is related to the rigid body's modes and tends to zero.

$$\frac{a}{F} = \Sigma_i \Sigma_j X_i X_j \frac{a_i}{F_j} \quad (6)$$

2.2 Theory of beam bending flexibility

A beam with basic supports at both ends and a force applied to the middle of the beam is shown bending in "Figure 1".

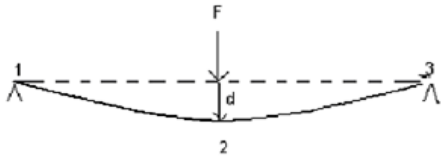

Figure 1: beam bending with two simple supports [18].

By taking the relation (7) into consideration, the coefficients are found.

F_2=F and X_2=1 (7)

The static balance equations also make it simple to obtain additional coefficients:

$$X_1 = X_3 = -\frac{1}{2} \Rightarrow F_1 = F_3 = -\frac{F_2}{2} \quad (8)$$

It is computed by changing the obtained values in the bending flexibility equation.

$$C_b = \frac{\Sigma_n X_n d_n}{F} \quad (9)$$

Ideally, d_1 and d_3 both go to zero. This formula corrects the circumstances for the rigid body's motion, even in the case of deformed supports. It is also possible to compute each mode of flexibility 's contribution in the following way:

$$C_b = \frac{\Sigma_i \Sigma_j X_i X_j \psi_i \psi_j}{m(2\pi f)^2} = \frac{(\psi_2 - \frac{\psi_1}{2} - \frac{\psi_3}{2})^2}{m(2\pi f)^2} \quad (10)$$

The above theory was a static theory in the calculation of flexibility. Now, through the modal theory, flexibility is investigated. Static flexibility follows the following standard formula:

$$C = \frac{Y}{F} = \frac{L^3}{48EI} \quad (11)$$

where L is the length of the beam, E is Young's modulus of the material used in the beam, and I is the inertia of the cross section of the beam. The

[DOI: 10.22068/ase.2024.680]

mode shape of the beam in the free state is according to equation (12) [18]:

$$y(x) = \frac{1}{2}\{\cosh(kx) + \cos(kx) - \frac{\sinh(kl)+\sin(kl)}{\cosh(kl)-\cos(kl)}[\sinh(kx) + \sin(kx)]\} \quad (12)$$

where y (0) = y(L) = 1, the modes' shapes are normalized, and k is a non-zero response that is determined by solving the equation $\cos(kl) = \frac{1}{\cosh(kl)}$. With a reasonable degree of accuracy, the values of k for the nth bending mode are as follows:

$$K_n = \frac{(2n+1)\Pi}{2}\frac{1}{l} \quad (13)$$

The following relation can also be used to determine resonance frequencies:

$$F = \frac{1}{2\pi}\left[\frac{EI}{\rho}\right]^{\frac{1}{2}} K^2 = \frac{1}{2\pi}\left[\frac{EI}{\rho}\right]^{\frac{1}{2}}\left[\frac{(2n+1)\pi}{2l}\right]^2 \quad (14)$$

where ρ is the mass per unit length (M/L) and M is the total mass. The modal mass (m) is calculated from the square integral of the modes and is necessarily equal to a quarter of the total mass of all bending modes:

$$m = \rho\int_0^l y(x)^2 dx = \frac{\rho l}{4} = \frac{M}{4} \quad (15)$$

The first forms of bending modes at the place of support and the place of application of load are as follows:

$$Y(0) = y(l) = 1, \quad Y\left(\frac{l}{2}\right) = -0.6078 \quad (16)$$

and by replacing them in the modal elasticity equation, we will have:

$$C_1 = \frac{\left(\frac{1}{2}+\frac{1}{2}+0.6078\right)^2}{(2\pi f)^2 m} = \frac{l^3}{48EI} \quad (17)$$

This relationship implies that the initial bending mode inevitably affects the bending flexibility. Since there will be no expression that contains the square of the modes, the second mode's and other even modes' contributions will be zero. The following will be the proportion of the third and fifth modes:

$$C_3 = \frac{1}{4352}\frac{L^3}{EI} \qquad C_5 = \frac{1}{7649}\frac{L^3}{EI} \quad (18)$$

The contribution of the third mode is extremely low. The contribution of the fifth mode is also very low due to its high frequency. A similar situation is also considered for individual higher modes, with the result that the first bending mode governs the flexibility of the structure when the load is applied to the middle of the structure. It is interesting to note that the change of the static shape in the structure is the same as the first shape of the bending mode of the structure.

2.3 Torsional Flexibility

The twist of a rectangular frame is shown in Figure 2. The frame is set on the supports at points 2 and 3, and the load is applied at points 1 and 4.

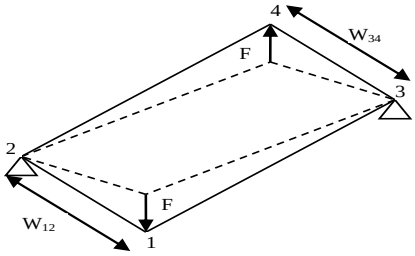

Figure 2: the frame twisting as a result of applying force [18].

In this case, the forces create a torsional couple Γ, and the applied forces and the reaction also come from the following relationships:

$$F_i = X_i\boldsymbol{\Gamma} \quad (19)$$

$$X_1 = \frac{\mathbf{1}}{\mathbf{w_{12}}} = -\mathbf{X_2} \qquad X_3 = -\frac{\mathbf{1}}{\mathbf{W34}} = -\mathbf{X_4} \quad (20)$$

Assuming small twist angles, the twist angle of the frame in radians is as follows:

$$\boldsymbol{\Omega} = \frac{\mathbf{d_1}-\mathbf{d_2}}{\mathbf{w_{12}}} - \frac{\mathbf{d_3}-\mathbf{d_4}}{\mathbf{w_{34}}} = \boldsymbol{\Sigma_i X_i d_i} \quad (21)$$

As a result, torsional flexibility in terms of Nm/rad is:

$$T = \frac{\boldsymbol{\Omega}}{\boldsymbol{\Gamma}} = \frac{\boldsymbol{\Sigma_i X_i d_i}}{\boldsymbol{\Gamma}} \quad (22)$$

The contribution of each specific mode of torsional flexibility can be written as follows:

$$\boldsymbol{\tau} = \frac{\boldsymbol{\Sigma_i\Sigma_j X_i X_j \psi_i \psi_j}}{\mathbf{m(2\pi f)^2}} = \frac{\boldsymbol{\Sigma_i X_i U_i^2}}{\mathbf{m(2\pi f)^2}} = \frac{\mathbf{1}}{\mathbf{m(2\pi f)^2}}\left(\frac{\boldsymbol{\psi_1}-\boldsymbol{\psi_2}}{\mathbf{w_{12}}} - \frac{\boldsymbol{\psi_3}-\boldsymbol{\psi_4}}{\mathbf{w_{34}}}\right) \quad (23)$$

Next, the frame is supported from three corners, while a load is supplied to the frame from the fourth corner to conduct the static torsion test.

[DOI: 10.22068/ase.2024.680]

The following is the determination of the static torsional stiffness based on the force-displacement curve [18].

$$T = \frac{\Omega}{\Gamma} = \frac{\Sigma_i X_i d_i}{\Gamma} \quad (24)$$

2. Method

3.1. Modelling

A Cad model of a bus was modeled by SolidWorks software. The bus body model is meshed in HyperMesh software. In this process, two-dimensional shell elements (triangular and quadrilateral) with an element size of 50 millimeters are employed. The constituent material of the bus body is steel, with specifications as outlined in "Table 1''. Figure 3 provides a comprehensive view of the finite element model of the BIW (body-in-white) components. Welded connections using RBE2 rigid elements interconnect the body components. The locations of these rigid welds are illustrated in Figure 4.

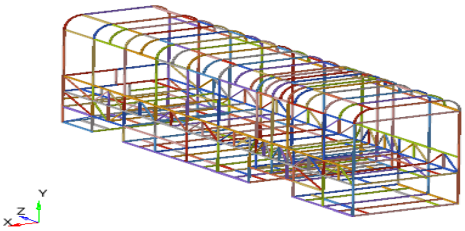

Figure 3: Full bus finite element model

Figure 4: Bus rigid welding RBE2

Table 1: Material properties

Steel	
Young's Modulus(E)	210000Mpa
Poisson's Ratio (v)	0.3
Yield stress (σy)	240Mpa
Density (ρ)	7.9e-9 tones/mm^3

The finite element model consists of 62112 elements and 244 components. Information related to the finite element model of the bus is presented in Table 2.

Table 2: elements data

Finite element model	
Two-dimensional shell element	62112
Rigid element	910
Node	64182

The HyperMesh program has evaluated the elements' quality and fixed any issues that were present in the model. In Table 3, the quality of the elements is provided.

Table 3: Elements quality

Quality item	No. of failed elements	Of failed elements %
Warpage>5	0 of 62112	0%
Aspect ratio>5	15 of 62112	0%
Skew>60	0 of 62112	0%
Jacobian<0.7	11 of 62112	0%

3.2. Loads and boundary conditions

3.2.1 Bending

Figure 5 shows that the bus body is restricted to 123, meaning that the x, y, and z directions are fixed. Boundary conditions were applied in place of the tires on the axle And all the boundary conditions are limited in 123. As shown in Figure 5, vertical loads imposed as pressure loads in the middle of the bus body have a value of 10,000 N.

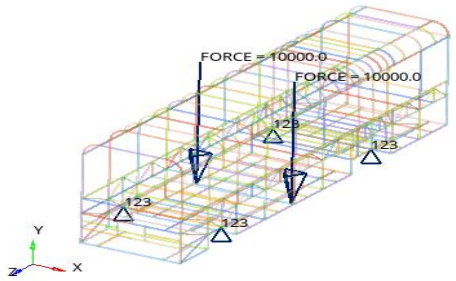

Figure 5: Boundary conditions and loads for bending analysis

3.2.2 Torsional

For torsional stiffness analysis, the bus body is limited to 3 and also 123. One of the boundary

[DOI: 10.22068/ase.2024.680]

conditions was imposed at the center of the front axle of the bus limited in 3, and the other was applied at the rear axle limited in 123. A force coupling is applied to the front axle, which is 10,000 N, as shown in Figure 6.

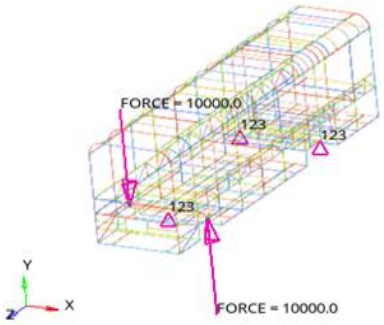

Figure 6: Boundary conditions and loads for torsional analysis

According to [4], these boundary conditions and forces are loaded.

3. Modal analysis

Modal analysis is a process in which the mechanical properties of a structure, including natural frequency, damping coefficient, and different mode shapes, are discussed. The first six modes are rigid modes, and the value in them is almost zero. Modal analysis is used to measure the dynamic response of structures when they are subjected to acceleration [19]. In this research, modal analysis is used to ensure connections and parts. Figures 7 to 9 show the shape of the bus mode in different modes. In the simplest case, where the material is linear elastic and follows Hooke's Law, the matrix equations can be represented as a dynamic three-dimensional spring mass system. The following is the generalized equation of motion [20]:

$$[M]\left[\ddot{U}\right] + [C]\left[\dot{U}\right] + [K][U] = [F] \quad (25)$$

where $[M]$ is mass matrix, $[C]$ is a damping matrix, $[K]$ is the stiffness matrix, $[U]$ is displacement, $[F]$ is the force vector. The overall issue is a quadratic eigenvalue problem with nonzero damping. However, the damping is typically disregarded for vibrational modal analysis, leaving only the first and third terms on the left:

$$[M]\left[\ddot{U}\right] + [K][U] = 0 \quad (26)$$

This is the typical eigensystem form that is used in FEM structural engineering. Harmonic motion is assumed to represent the free-vibration solutions of the structure [21]. According to this presumption, $\left[\ddot{U}\right]$ is taken to equal $\lambda[U]$, where λ is an eigenvalue (with units of reciprocal time squared, e.g., s^{-2}) Using this, the equation reduces to [20]:

$$[M]\lambda[U] + [K][U] = 0 \quad (27)$$

On the other hand, the static problem equation is:

$$[K][U] = F \quad (28)$$

This is anticipated when all time derivative terms are set to zero. Table 4 shows the first ten frequency modes after the six rigid modes.

Table 4: Ten modes of frequency

Mode	Frequency (Hz)
1	1.919111
2	2.551669
3	3.086311
4	3.745976
5	4.173711
6	4.515196
7	4.786030
8	4.982533
9	5.340010
10	5.633844

[DOI: 10.22068/ase.2024.680]

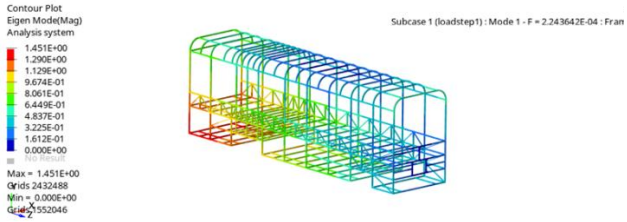

Figure 7: Bus first frequency mode

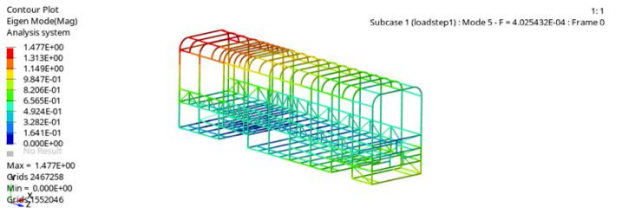

Figure 8: Bus fifth-frequency mode

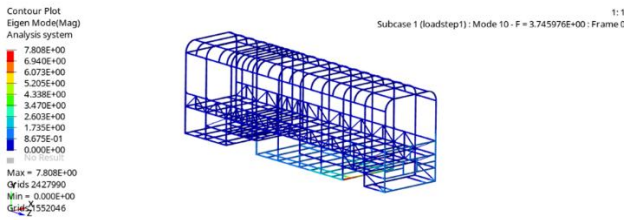

Figure 9: Bus tenth frequency mode

5. Results

The displacement and stress of the body frame under bending conditions are shown in Figure 10(a) and 10(b). The side walls of the bus and the lower beams experience a maximum von Mises stress of 275 Mpa due to the bus's structural design, which exceeds the yield strength of steel. This indicates that these components lack sufficient strength to withstand bending in the bus.The high-stress area is framed in the middle and back. The main reason is that the engine and gearbox of the bus are located in this area. This is similar to [5] in which the maximum stress is concentrated in the middle and back of the bus body. According to the figure 10(a), it can be seen that the vertical displacement is located at the junction of the luggage compartment, engine, and gearbox. This is also similar to the result of [5].

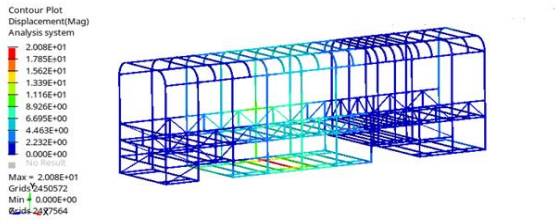

Figure 10(a): Displacement due to vertical bending

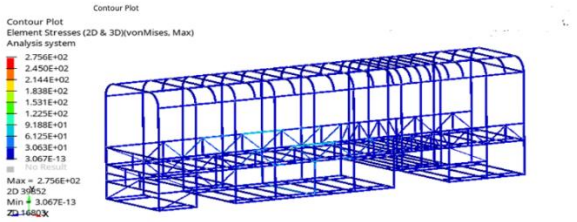

Figure 10(b): Von mises stress due to vertical bending

$$K_b = \frac{F}{\delta} = 1638.672676 \text{N/mm} \quad (29)$$

In equation (29), k_b is the bending stiffness, and F is the applied force, δ is the maximum displacement [5]. A measure used to evaluate a bus structure's bending or deflection after torque is applied is called torsional stiffness. It should be enhanced to the point where the bus cannot twist under the different torsion loadings that the vehicle is subjected to [4]. The displacement and stress of the body frame under constrained torsional circumstances are shown in Figure 11. The tension generated by the luggage compartment and the frame beam results in the maximum Von Mises stress 581 Mpa which exceeds the yield strength of steel. This indicates that these components lack sufficient strength to withstand bending in the bus, as shown in Figure 11(a). this result also is similar to [5]. The peak of the dashed line and the wind window are where the highest displacement is found, as shown in Figure 11(b). The front wheel suspension is the reason for this issue.

[DOI: 10.22068/ase.2024.680]

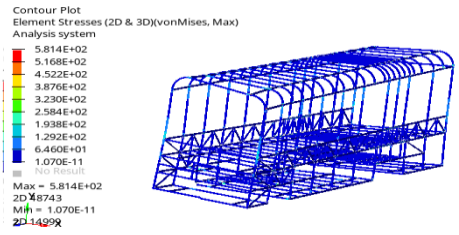

Figure 11(a): Von Mises stress due to torsional

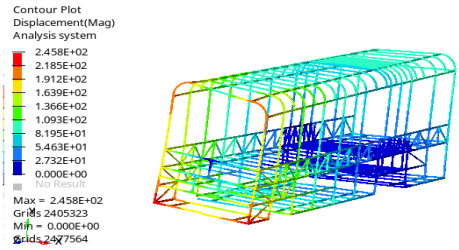

Figure 11(b): Displacement due to torsional

$$K_t = \frac{T}{\varphi} = \frac{F*t}{arctan(\frac{\delta}{t})} = 1023890.78 \text{N.mm/°} \qquad (30)$$

In equation (30), k_t is torsional stiffness, T is torque moment, and φ is torsional angle [5].

4. Discussion

The main source of external stimulation for a bus travelling on a roadway is uneven surface. The highest frequency of road excitation, according to pertinent data, is between two to five Hz. Another significant external source of excitation is engine excitation. The engine usually runs at 600–800 rpm when it is inactive, and the vibration frequency is typically 30–40 Hz. Resonance won't happen since the bus's first ten-order natural frequency spans 1.9 Hz to 5.63 Hz. One of the important limitations of this study was the size of the structure, which required a strong system to solve it in a short period of time.

5. Conclusions

The torsion analysis results demonstrate that the bending stiffness is 1638.672676N/mm and the torsional stiffness is 1023890.78N.mm/°. The optimum analysis of multiple different cars indicates that for economical sedans, the body's torsional stiffness and windshield stiffness range mainly between 700 and 900. This ranges from 900 to 1300 N*mm/rad for mid-size automobiles. In general, an automobile's torsional rigidity increases with size. In general, the bending stiffness of BIW for medium cars, SUVs, and economical sedans is approximately 1000, 13000, and 12,000 N/mm. The torsional and bending stiffness values that were found are both greater than these values. The bus body's torsional and bending analysis results, which are displayed in figures 8 and 9, indicate that the front axle's suspension system caused the maximum displacement in torsion to occur in the bus's dashed line near the front window, and the connection point between the engine and luggage and gearbox caused the maximum displacement in bending. Due to the engine and gearbox, the bus's side walls and bottom beams have the highest Von Mises stress in bending, and the luggage has the highest Von Mises stress in torsional stress. Modal analysis has been analyzed in the first ten modes, and according to what was stated in the discussion section, resonance does not occur according to the values of the first ten modes of the bus body. The accuracy of the obtained data is confirmed by comparing the location of the highest stress and displacement in the torsional and bending stiffness [5].

List of symbols

E	Modulus of elasticity
k	Stiffness
ν	Poisson's Ratio
σ_y	Yield stress
ρ	Density
T	Torque moment
ϕ	Torsional angle
δ	Displacement
F	Applied force

[DOI: 10.22068/ase.2024.680]

References

[1] Jing, K., Chen, J.X. and Wu, J., 2018. Modal Analysis of Bus Body Frame Based on Hyperworks. Journal of Agricutural Equipment & Technology. 2, pp.54-57.

[2] Yin, Z.P., 2007. Finite Element Analysis and Test Investigation for XQ6125 City Bus. D. Shanghai: Shanghai Jiao Tong University. Conf. Ser. 1748 062073

[3] Jain, R., Tandon, P. and Vasantha Kumar, M., 2014. Optimization Methodology for Beam Gauges of the Bus Body for Weight Reduction. Journal of Applied and Computational Mechanics. pp.47–62.

[4] Izanloo, M. and Khalkhali, A., 2017. Analysis of Torsional and Bending Stiffness of a Sedan Vehicle Using Simplified Finite Element Model. Journal of Solid and Fluid Mechanics. 7(2), pp.17-26.

[5] Yao, C. and Yang, M., 2021. Analysis of Strength Stiffness and Modes for Bus Body Frame. In Journal of Physics: IOP Conference Series, IOP Publishing. 1748.

[6] Iozsa, M.D., David, V.C. and Manea, A.M., 2019, October. The Influence of the Roof Frame on the Stiffness of a Bus Structure. In IOP Conference Series: Materials Science and Engineering, IOP Publishing. 564.

[7] Iozsa, M.D., David, V.C. and Manea, A.M., 2018, November. Effect of Side Stiffening Plates on the Stiffness of the Bus Structure. In IOP Conference Series: Materials Science and Engineering, IOP Publishing. 444.

[8] Patel, T.M. and Bhatt, N.M., 2015. Finite Element Analysis of Automobile Structural Member Using Ansys. GIT-Journal of Engineering and Technology, 8(1), pp.1-10.

[9] Kurdi, O., Rahman, R.A., Samin, P.M., Yob, M.S., Nadarajan, N.K. and Yulianti, I., 2017. Torsional Stiffness Improvement of Truck Chassis Using Finite Element Method. Rotasi, 19(2), pp.76-81.

[10] Naseri, R. and Mohammadzadeh, S., 2020. Nonlinear Train-Track-Bridge Interaction With Unsupported Sleeper Group. International Journal of Railway Research, 7(1), pp.11-28.

[11] Kabir, M.M., Izanloo, M. and Khalkhali, A., 2017. Concept Design of Vehicle Structure for the Purpose of Computing Torsional and Bending Stiffness. International Journal of Automot Eng. 7, pp. 2370-2377.

[12] Addisu, H.S. Koricho, E.G., 2022. "Structural Weight and Stiffness Optimization of a Midibus Using the Reinforcement and Response Surface Optimization (RSO) Method in Static Condition". Journal of Modelling and Simulation in Engineering, Article ID 6812744.

[13] Kawade, R.K. and Mohan, N., 2015. Chassis Frame Torsional Stiffness Analysis. International Journal for Scientific Research & Development. 3, pp.312-315.

[14] Naseri, R., Mohammadzadeh, S. and Rizos, D.C., 2024. Rail Surface Spot Irregularity Effects in Vehicle-Track Interaction Simulations of Train-Track-Bridge Interaction. Journal of Vibration and Control 2024.

[15] Gamea, T. and Melsew, A., 2022. Numerical Investigation of Dynamic Analysis of Bus Structure. journal of Global scientific. 10(6), pp.439-450.

[16] Sreenath, S. and Kamalakkannan, K., 2016. Design and Analysis of a Bus Body Side Frame. International Journal of Mechanical And Production Engineering. 4(4).

[17] Marzbanrad, J. Hafezian, M. and Mozaffarikhah, M. (2017), Heavy Trucks, Technology And Troubleshooting, K. N. Toosi University Publications.

[DOI: 10.22068/ase.2024.680]

[18] Arfken, G.B., Weber, H.J. and Harris, F.E., 2011. Mathematical Methods for Physicists: a comprehensive guide. Academic press. 27.

[19] Deulgaonkar, V.R., Kulkarni, M.S., Khedkar, S.S., Kharosekar, S.U. and Sadavarte, V.U., 2020. Modal Analysis of Bus Body Structure Using Finite Element Analysis Technique. International Journal of Vehicle Structures & Systems (IJVSS), 12(3).

[20] Ray W, C. and Joseph, P. Dynamics of Structures, 2nd Ed., McGraw-Hill Publishing Company, New York, 1993

[21] Bathe, K.J., 2006. Finite Element Procedures. Klaus-Jurgen Bathe, 2nd Ed., Prentice-Hall Inc., New Jersey, 1996.

[DOI: 10.22068/ase.2024.680]